



Computational modelling and analysis of heat transfer enhancement in straight circular pipe with pulsating flow

S. V. Nishandar¹ · A. T. Pise² · P. M. Bagade³ · Mahendra U. Gaikwad⁴ · Amanpreet Singh⁵

Received: 24 January 2024 / Accepted: 12 May 2024

© The Author(s), under exclusive licence to Springer-Verlag France SAS, part of Springer Nature 2024

Abstract

A thorough grasp of the complex dynamics of pulsing flow is essential for improving heat transfer processes and creating effective systems, especially in situations where pulsations play a crucial role. Because pulsing flow has so many engineering applications, it has attracted a lot of attention when it comes to improving heat transmission. In this work, we examine several important factors influencing the properties of heat transmission, such as the Reynolds number (Re), length (L), diameter (D), frequency (f), and pulsation amplitude (A) of the pipe. All the results reported are for $3 - D$ configuration. Regarding turbulent kinetic energy (TKE), the mechanism is clarified for the various characteristics that are taken into consideration. The present work reports the results for a varied range of turbulent Re with different A , f , L and D . The impact of alterations of these parameters on its heat transmission properties is scrutinized. Also the TKE analysis is reported which provides insight into flow development and its effects on the heat transfer enhancement. It has been found that, in contrast to low frequencies, higher frequency pulsing velocity inputs boost the local Nusselt number (Nu) by penetrating the domain at a greater distance. Computational simulations using ANSYS Fluent are used to study a range of sinusoidal pulsating velocity inputs with different A s and f s. The present study highlights how crucial it is to comprehend pulsating flow dynamics in order to optimize heat transfer procedures and create effective systems for use in engineering applications. It is advised to investigate a larger range of parameters in order to find the best mixes of f s and A s for increased heat transfer efficiency.

Keywords Heat transfer enhancement · Pulsating flow · Turbulent flow · Numerical heat transfer

1 Introduction

The crux of interactive design and manufacturing (IDM) lies in the utilization of digital technology, design and manufacturing processes to facilitate iterative improvements throughout the product development lifecycle. On the other side, computational analysis of the pulsating heat transfer through CFD approach provides insights into the details of the flow field and physics. Such detailed analysis can be of great help using IDM in the design and optimization of heat transfer systems. Heat exchangers and cooling systems are a couple of examples of heat transfer components that can be optimized using these simulations to increase performance

A. T. Pise and Amanpreet Singh have authors contributed equally to this work.

✉ P. M. Bagade
pramodbagade@gmail.com

✉ Mahendra U. Gaikwad
mahendragaikwada1@gmail.com

S. V. Nishandar
siddhant.nishandar04@gmail.com

A. T. Pise
ashokpise@gmail.com

Amanpreet Singh
preetam70@gmail.com

¹ Department of Mechanical Engineering, Govt. College of Engineering Karad, Shivaji University, Kolhapur, M.S. 415414, India

² Department of Mechanical Engineering, Govt. College of Engineering, Karad, Shivaji University, Kolhapur, M.S. 414414, India

³ Department of Mechanical Engineering, TSSM's BSCOER, Narhe, Pune, M.S. 411041, India

⁴ Department of Mechanical Engineering, JSPM's, Narhe Technical Campus, Pune, M.S. 411041, India

⁵ Center for Research Impact and Outcome, Chitkara University, Rajpura, Punjab 140401, India

and efficiency. It is noted that the effect of the pulsation sustains in a part of the flow domain, and a major part near the outlet does not get affected by this pulsations adequately. Turbulent kinetic energy (TKE) analysis has been performed to explain this mechanism. It is noted from literature that during many heat transfer system employ uniform fluid flow configuration. These are also used in micro-channel applications also. Investigations of such systems provide input about single and two-phase system behaviour during heat transfer process [15, 34, 41, 44, 85].

Besides the uniform flow system, many applications are found, where pulsating and oscillating flows have been incorporated for heat transfer enhancement. It is well-accepted that during pulsating flow, the time-averaged velocity component is non-zero. This characteristic of pulsating flow makes it a distinguished case for investigation of heat transfer enhancement possibilities. Such flows are defined by f and A of the pulsating flows. Despite of several studies in this area, there has not been a common consensus on whether pulsating actually helps heat transfer enhancement or not and still remains a topic for further research. Havemann and Narayan Rao [32] conducted investigations on the heat transfer via heated pulsating air, flowing in a horizontal circular pipe in the range of $5000 \leq Re \leq 35,000$. They reported 30% change in Nu with varying frequency (f), amplitude (A), wave-forms and Re . It was noted that the critical frequency mainly depends on the wave-form and Re does not make a significant effect. The exact nature of this function was not established. Since then, various investigations were undertaken to understand the pulsating heat transfer (PHT). During such flows, there is a periodic behaviour of mass flow rate and the pressure gradients. For a case of flow through a pipe, it may be considered as superposition of pulsating or oscillating component over a steady Poiseuille flow. Since many of the practical fluid flow applications in a pipe are in the domain of turbulent flow regime, much attention has been given in this area. However, the research reported in literature expands in a narrow region of operating variables and hence conflicting results appear in literature. Some authors Cumpsty and Greitzer [18], Esfe et al. [23], Metwally [53], Mladin and Zumbrennen [55], Nabavi [58, 59], Sheriff and Zumbrennen [69], Tesa and Trávníček [76], Wagshul et al. [77], Yuan et al. [86] claim to see the enhancement in heat transfer, while some researchers Akdag and Ozdemir [1, 2], Akdag and Ozguc [3], Chen et al. [16], Ghafarian, Mohebbi-Kalhari, and Sadegi [27], Leong and Jin [46], Wu et al. [82], Xiao et al. [83], Zhao and Cheng [87] reported adverse results. In the present study, various parameters affecting PHT flow in circular pipe are investigated. It has been observed by many researchers Ye et al. [84] and references therein that heat transfer increases with increased Re , f and A . However, for unidirectional the heat transfer enhancement was limited to 20% for specific range of these parameters. For example, Kikuchi et al. [44]

conducted experiments at $Re = 400$ and pulsating Strouhal number ranging from 0 to 1.37.

Khosravi-Bizhaem et al. [43] reported 19% rise in overall heat transfer coefficient at $f = 4$ Hz. The experiments were conducted in the Re range of $2000 < Re < 9600$ and frequency range of $2 < f < 10$ Hz. The authors reported that heat transfer tends to a steady flow at higher frequency. The available literature indicates that there is a need for rigorous analysis of heat transfer enhancement in turbulent region, hence the Re range is selected between $10,000 < Re < 20,000$ for the present research. Other parameters like A , f are chosen referring to the literature Kikuchi et al. [44], Mohammed et al. [6], Ye et al. [84]. For the chosen Re , the entrance length comes out to be 0.5 m. It is very necessary to capture the effects of entrance length for the developing flow. Many researchers have not explicitly considered this factor, which is now considered in our research. Also, a limited literature available where the heat transfer enhancement is investigated with reference to evolution and distribution of turbulent kinetic energy, which we have reported in the present work. In turbomachinery blade cooling applications, the typical Re ranges between $10,000 \leq Re \leq 80,000$ Han and Chen [30].

Owing to versatile applications and importance of pulsating flows in several engineering domains, it has been a topic of great interest for researchers. Pulsating flows, specifically for heat transfer enhancement has been widely investigated, e.g. aerospace engineering Nobrega et al. [61], biomedical engineering Babu et al. [8], micro-channel heat sinks for electronics application Persoons et al. [62], Singh et al. [72], IC engines Plotnikov [63], modular electronics cooling Hota et al. [37], Constantinou et al. [17], biomimetic microchannels Daba et al. [19] are recent studies carried for the investigating pulsating heat flows. At the same time, many researchers have focused on the role of turbulence and TKE in heat transfer enhancement Fan et al. [24], Bergman et al. [12, 13], Tanda [74], Wilcox et al. [79] for possible applications in industry also from theoretical point of view. Kholi et al. [42] employed Artificial Neural Network (ANN) for improved performance predictions. Khandekar et al. [40] have reported IDM aspect of pulsating heat pipes with reference to thermal management of engines and machinery. Wu et al. [81] reported effects of the gravitational direction, inner diameter, and filling ratio on the startup characteristics of PHPs and noted that smaller rise in temperature was recorded for shorter pulsation. Mu et al. [57] have reported possible use of IDM in pulsating heat transfer applications. They observed that many components will malfunction or perhaps be destroyed due to heat generated during operation if there is insufficient heat dissipation capacity. Pulsating heat pipes that offers numerous benefits have drawn the interest of numerous academics and demonstrated significant promise in the field of thermal management. These are the greatest option for cooling electronic equipment due to their high

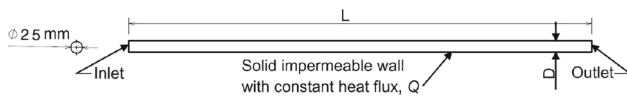


Fig. 1 Schematic of numerical setup

heat flux conditions, stable operation, and capacity for heat exchange.

With pulsing heat transfer methods, there are many opportunities for innovation in industrial processes and sectors. Manufacturers can leverage the unique properties of pulsed heat transfer, such as higher heat transfer rates and compact device designs, to improve the efficiency, reliability, and sustainability of their operations. By looking into a range of applications, such as Advanced Cooling Solutions in Additive Manufacturing Magerramova et al. [51], Compact Thermal Management Systems in Electronics Production Lohrasbi et al. [49], and spacecraft thermal control Hengeveld et al. [35], industries can significantly increase productivity, efficiency, and product quality. Additionally, these applications have the potential to significantly increase efficiency by incorporating pulsing heat transfer mechanisms into manufacturing processes. Schematic of the numerical setup used during present study is shown in Fig. 1. Effects of these parameters on the heat transfer characteristics are discussed in Sect. 4.

2 Literature review

Yu et al. [85] analytically investigated convective heat transfer in a circular tube with constant heat flux for a pulsating laminar flow and found out that the solution (temperature and the mean Nusselt number, Nu) deviate about steady state laminar convection solution periodically. The authors reported that the Nu depends on pulsation frequency (f), amplitude, (A), and the Prandtl number, (Pr). Experimental studies by Zohir et al. [88] examined the heat transfer for laminar and turbulent pulsating pipe flows under various Re , f , pulsator location, and tube diameters (D) configurations, under uniform heat flux. Their results showed the effects for $750 \leq Re \leq 12,320$ and the pulsation frequency, $1 \leq f \leq 10$ Hz. The authors also reported that for a greater Res ($8000 \leq Re \leq 12,000$), the heat transfer rate was enhanced for larger pipe diameters. An oscillating SHM was employed during experiments by Gerrard [26] on a pipe flow at $Re = 3770$. Their focus was on the turbulent transition regime and Re was chosen accordingly to understand laminarization under the applied conditions. The authors noted that the laminarization significantly contributes to the oscillation component and recommended extending the findings to greater Res and other frequencies. Computation of solitons with high order numerical schemes was reported by Ashwin et al. [7].

Jun et al. [38] reported the effects of pulsation on the rate of heat transfer. Heat transport was investigated in relation to hydrodynamic parameters and pulsation features. Their findings showed that the hydrodynamic characteristics and resonator configuration both affect the rate of heat transmission and there is a perfect length at which the heat transfer improvement works best. Also, the hydrodynamic parameters and the pulsing properties improved heat transfer during their investigation. He and Jackson [33] explored pulsing turbulent flow in a conduit at frequencies between 0.004 and 0.04 in another experimental research. The size of this zone shrinks when the pulse frequency is decreased, eventually ceasing to “freeze”. The researchers found that the frozen region shrinks as the frequency is increased. The flow in the core region displayed a ‘frozen’ behavior, with insignificant changes in velocity in the core. It was discovered that the wall region is where the influence of turbulence to an enforced pulse of flow rate first manifests itself before spreading into and across the core. As a result, the turbulent fluctuation in the core region responded with a time delay that increases with distance from the wall. During the pulsating cycle, the inflection point instability is noted by [54]. The flow and heat transfer in a circular tube under sinusoidally pulsing flow conditions in the laminar regime were numerically examined by [14]. The authors reported no effect on time-averaged heat transfer, although at the near-entry zone, Nu distribution varies with time.

Guo and Sung [29] conducted a series of experiments to determine the heat transfer characteristics for pulsating flow in a circular pipe and reported favourable effects of f and A on heat transfer enhancement. In this investigation, the large amplitude of the pulse flow rate ($A_f \geq 1$) received the most attention. Depending on the pulsation frequency, both heat transfer augmentation and reduction for a small amplitude ($0 \leq A_f \leq 1$) were recorded. According to the authors, the heat transfer caused by pulsation is usually increased for large amplitudes ($A_f \geq 1$). Gbadebo et al. [25] reported an empirical correlation between Nu_{local} and Nu_{avg} for steady and pulsating flows in a pipe. They used experimental data heated pipe with uniform heat flux. During experiments by Mackley et al. [50] on lubricating oil flow through heat exchanger, a considerable increase in Nu was recorded with both the flow oscillation and baffles present. The scientists emphasized that in the studied range, fluid oscillation alone had no impact on heat transfer. But when baffles were used, the impact was tremendous. According to Nishandar et al. [60], Nu_{mean} values increase with pulsation, but Nu_{local} values either rise or fall as the pulsation frequency increases. The authors proposed that placing the pulsing mechanism downstream is the most efficient strategy to raise the average heat transfer coefficient.

Elshafei et al. [21] conducted heat transfer investigation in a pipe, throughout the range of $10^4 \leq Re \leq 4 \times 10^4$ and 0

$\leq f \leq 70$. In comparison to steady flow, their results showed a small decline in the interim average, and for fully established, established regions, the local values either grew or fell relative to steady flow values. The frequency parameter was discovered to be a factor in *Nu* local variation. Similar experimental investigations are reported by Gül [28], with oscillating frequencies between $5 \leq f \leq 100$ Hz and spanning a range of $10 \times 10^3 \leq Re \leq 5 \times 10^4$. The oscillating frequency, f , and Re showed a significant impact on Nu , while this effect was dominant in entrance region. Additionally, Moschandreou and Zamir [56] reported favourable effects of Pr and f . Their analysis describes a positive peak during the pulsation, which increases the bulk temperature of the fluid and Nu for a moderate frequency values. However, the effect is reversed when the frequency is outside of this range. Higher peaks were noted for lower Pr .

Another experimental study by Elshafei et al. [22] established the influence of Nu by f and resonance energy. They discovered that, the *Numean* may rise or fall depending on the frequency range. The classification of heat transmission according to the turbulent bursting model was also reported by the authors. Effect of large fluctuating amplitudes on heat transfer was numerically examined by Wang and Zang [78]. Their findings suggest that Womersley number (Wo) defines the pulsating heat transfer to a great extent. At a specific Wo , higher amplitude of oscillation and flow reversal is noted improving the heat transfer. In a computational investigation of the pulsing flow and heat transfer characteristics in a tube whose diameter fluctuates often, Shu et al. [70] discovered that convergent-divergent tubes exhibit better heat transfer features than straight tubes. According to Targui and Kahalerras [75], A , f and permeability of the porous baffles all have an impact on the flow structure and heat exchanger performance. According to their findings, adding an oscillating component to a mean flow has an impact on the flow structure and improves heat transmission compared to a steady, non-pulsating flow.

Das et al. [65] investigated the characteristics of pressure drop and heat transfer in a pulsing channel flow caused by flexible flow modulators mounted on walls. Vorticity contours and isotherms were used to assess the system properties, while pressure drop across the channel and variations in Nu have been used to assess heat transfer performance. In another study by Hosseinalipour et al. [36], the authors reported that Nu and Se have a close relationship, as evidenced by the secondary flow intensity increasing with rotation and Res . Their analysis was made on a two-passage internal cooling channel model with a 180° U-turn at the hub portion at $Re = 10,000$. Heat transfer and pressure loss measurements were investigated representative internal cooling passage of a stationary engine over a range of $18,000 \leq Re \leq 105,000$ for three aspect ratios of a rectangular section by Ryley et al. [64]. One of a novel solution to overcome

issues related to high energy density devices using pulsing flow in single-phase cooling systems was reported by Alimohammadi et al. [5]. The authors investigated pulsing flows in a rectangular minichannel subjected to asymmetric sinusoidal flow pulsations both experimentally and numerically. Their study reports a notable improvement in heat transfer at larger amplitudes of pulsation flow rates, with an approximate 11% increase over constant flow circumstances. Sobhnamayan et al. [73] investigated the forced convection heat transfer and pulsing flow in a porous medium-filled pipe. Sierra-Vargas et al. [71], while studying the effects of Re on film cooling of gas turbine vanes found that the he jet trajectory and recirculation zones have a major influence on the film's effectiveness under adiabatic temperature conditions. They conducted their analysis in Re range of $3500 \leq Re \leq 11,000$. Alami et al. [4] in his study reported paradoxically inconsistency and a seemingly incomplete understanding of the convective heat transfer mechanism. Many researchers have contributed to the study of the mechanism behind the difficult problem of turbine blade cooling in turbomachinery applications. The normal Re in such cooling applications is between 10,000 and 80,000 Han and Chen [30]. A minimal degree of turbulence is anticipated in the nozzle staging of the turbine's first stage, but turbomachinery operates in a wide range of Re in various stages, as reported by Balje [10]. The available literature reveals that there are several important applications of pulsating fluid flow, where heat transfer enhancement needs attention. As noted in the literature survey above, the mechanism of convective heat transfer particularly in pulsating condition has not been addressed in a large Re range. Effects of entrance length, TKE are missing. Hence, the present research aims at providing some insights to these parameters through numerical investigation. The remaining part of current work is reported as follows. First, the governing equation required for $3 - D$ simulation with boundary conditions are discussed. Following this, the important parameters pertaining to convective heat transfer have been discussed. The details of the CFD analysis are reported in the next section. An emphasis is given to the TKE analysis, which is separately discussed in Sect. 3.4. The result for various cases are analysed in detail in Sect. 4, followed by the conclusions in Sect. 5. The future scope of present work is also mentioned in Sect. 6.

3 Methodology

The methodology followed during the present research is as follows:

It includes the derivation of governing equations, the determination of critical parameters, mesh production, boundary condition definition, and examination of the turbulent kinetic energy distribution. First the governing equations

are reported, which explain the basic ideas guiding fluid dynamics in the simulated environment. This is followed by explaining the crucial parameters in the present research. Identification and definition of key parameters influencing the system under investigation are important for a thorough analysis. In order to accurately represent the complexities of fluid flow phenomena, great care is taken to discretize the computational domain by creating a mesh and precisely defining boundary conditions. The analysis of TKE distribution is a key component of the investigation as it provides insight into the intensity of the turbulent flow and how it affects the overall behavior of the flow in the simulated environment, which is reported in the last subsection.

3.1 Governing equations

In this section, the governing equations, important parameters related to heat transfer for pulsating flow used in the present investigation are presented. The governing equations for the problem in the present research are the full 3 – D.

Navier–Stokes equation as given below:

$$\frac{\partial p}{\partial t} + \frac{\partial(\rho u)}{\partial x} + \frac{\partial(\rho v)}{\partial y} + \frac{\partial(\rho w)}{\partial z} = 0 \tag{1}$$

$$u \frac{\partial u}{\partial x} + v \frac{\partial u}{\partial y} + w \frac{\partial u}{\partial z} = -\frac{1}{\rho} \frac{\partial p}{\partial x} + \mu \left(\frac{\partial^2 u}{\partial x^2} + \frac{\partial^2 u}{\partial y^2} + \frac{\partial^2 u}{\partial z^2} \right) \tag{2}$$

$$u \frac{\partial v}{\partial x} + v \frac{\partial v}{\partial y} + w \frac{\partial v}{\partial z} = -\frac{1}{\rho} \frac{\partial p}{\partial y} + \mu \left(\frac{\partial^2 v}{\partial x^2} + \frac{\partial^2 v}{\partial y^2} + \frac{\partial^2 v}{\partial z^2} \right) \tag{3}$$

$$u \frac{\partial w}{\partial x} + v \frac{\partial w}{\partial y} + w \frac{\partial w}{\partial z} = -\frac{1}{\rho} \frac{\partial p}{\partial z} + \mu \left(\frac{\partial^2 w}{\partial x^2} + \frac{\partial^2 w}{\partial y^2} + \frac{\partial^2 w}{\partial z^2} \right) \tag{4}$$

Equation 1 represents the continuity equation, while Eqns. 2, 3 and 4 represent momentum equations in x-, y- and z- directions respectively. The TKE, (*k*) is given by Eq. 5, while for dissipation ϵ , Eq. 6 is used.

$$\frac{\partial p(\rho k)}{\partial t} + \frac{\partial(\rho k u_i)}{\partial x_i} = \frac{\partial}{\partial x_j} \left[\frac{\mu_t}{\sigma_k} \frac{\partial k}{\partial x_j} \right] + 2\mu_t E_{ij} E_{ij} - \rho \epsilon \tag{5}$$

$$\frac{\partial p(\rho \epsilon)}{\partial t} + \frac{\partial(\rho \epsilon u_i)}{\partial x_i} = \frac{\partial}{\partial x_j} \left[\frac{\mu_t}{\sigma_\epsilon} \frac{\partial \epsilon}{\partial x_j} \right] + C_{1s} \frac{\epsilon}{k} 2\mu_t E_{ij} E_{ij} - C_{2s} \rho \frac{\epsilon^2}{k} \tag{6}$$

$$\frac{\partial}{\partial x} \left(k \frac{\partial T}{\partial x} \right) + \frac{\partial}{\partial y} \left(k \frac{\partial T}{\partial y} \right) + \frac{\partial}{\partial z} \left(k \frac{\partial T}{\partial z} \right) + q_v = \rho C_p \frac{\partial T}{\partial t} \tag{7}$$

where, u_i = velocity component in corresponding direction, E_{ij} = component of rate of deformation and μ_t represents eddy viscosity. The energy equation is given by 7.

3.2 Important parameters

Various important parameters used in the present study are defined as follows:

Heat Transfer rate is given by Newton’s law of cooling Han and Wright [31],

$$Q = hA(T_w - T_b) \tag{8}$$

where, h is heat transfer coefficient, A is projected area, T_w is the local wall temperature and T_b is bulk temperature. Local heat transfer coefficient is given by Kern [39],

$$h_x = Q_{net}/(A(T_w - T_b)) \tag{9}$$

where, h_x is the local heat transfer coefficient, (Q_{net}/A) is the local heat transfer rate per unit from the wall to air inside of tube. Local Nusselt number Theodore et al. [12],

$$Nu_x = h_x D/k \tag{10}$$

In oscillatory flows, Re_{osc} can be characterised as given by Eq. 11 [28].

$$Re_{osc} = \frac{2\pi f x_o D}{V} \tag{11}$$

The friction factor was determined from the measured values of pressure drop, ΔP across the test length, L and mass flow rate, \dot{m} using the Eq. 12

$$f = \frac{\Delta P}{((L/D)\rho V^2/2)}; V = \frac{\dot{m}}{(\rho \pi D^2/4)} \tag{12}$$

Using the values obtained from the experimental data in the oscillating pipe, the changes various correlations between Nu and Re were established [28]. The following are important from the subject point of view. We have used Dittus-Boelter equation for the calculation of theoretical Nu , as given by Eq. 13, which describing the smooth tube flow without oscillation. There is broad acceptance of the Dittus-Boelter empirical correlation Dittus and Boelter [20], McAdams [52], Winterton [80] for predicting the Nusselt number with turbulent flow in smooth-surface tubes.

$$Nu = 0.023 Re^{0.8} Pr \tag{13}$$

3.3 Meshing and boundary conditions

Mesh generation is one of the most important step in the whole simulation process. It has been well demonstrated that the grid (mesh) quality significantly affect the accuracy of the solution. An in-depth discussion on the efficacy of a

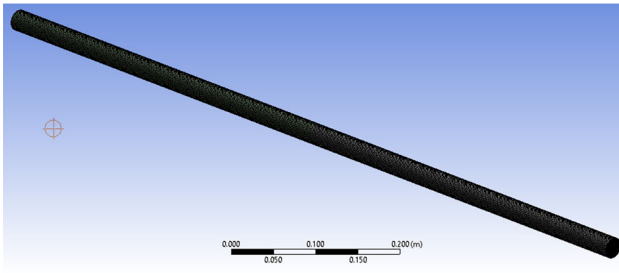


Fig. 2 Mesh on the full model

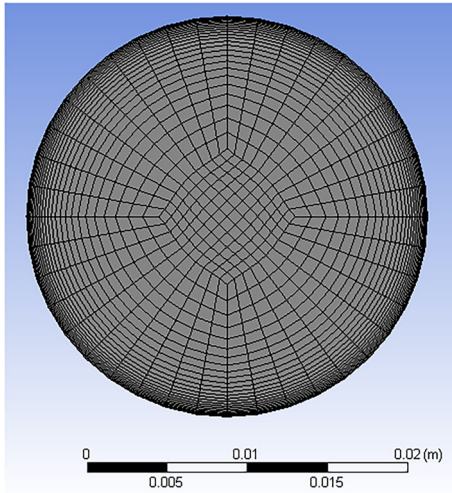


Fig. 3 Meshing as seen on the cross section of the pipe

high quality grid and its effects on the solution are reported in Bagade et al. [9]. Authors noted that orthogonal grids provides the most accurate solution. Hence, in the present research work, we have tried to generate the mesh which will be very close to orthogonality. To capture the wall and heat transfer effects a very refined grid spacing is employed ($y^+ = 0.5$, $y = 1.3628 \times 10^{-5}$). It is well established fact that one has to work with a very fine grid size, specifically near wall to capture viscous and heat transfer effects. Hence, it is imperative to first calculate the appropriate grid size. In the present work, all the grids are generated with a numerical wall spacing $y^+ \sim 1$. The wall normal distance is calculated as $y = \frac{y^+ \mu}{u_\tau \rho}$, where μ is coefficient of viscosity, ρ is density and u_τ is shear velocity. Hence first shear velocity is calculated, which is given as $u_\tau = \sqrt{\frac{\tau_w}{\rho}}$, where τ_w is wall shear stress. Wall shear stress is calculated as $\tau_w = \frac{c_f}{2} \rho U_\infty^2$. c_f is coefficient of friction and is a function of Re . It is calculated as $\frac{c_f}{2} = 0.039/Re^{1/4}$. This process is employed for calculating the wall resolution required for different Re keeping wall resolution at approximately 1×10^{-5} . The grid thus created has 1,283,136 nodes (Figs. 2 and 3). At inlet of the pipe, two different velocity inputs were given. For the validation of the

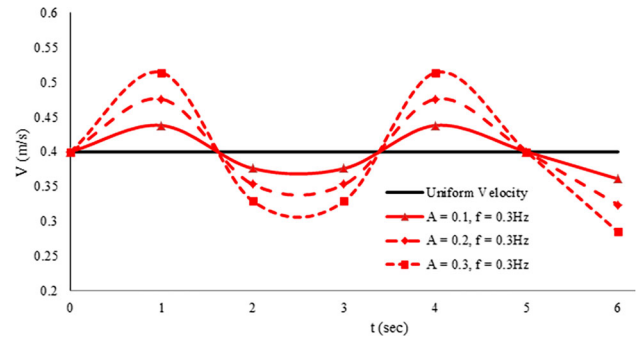


Fig. 4 Sinusoidal pulsating velocity inputs with the different pulsation amplitude, A and $f = 0.3$

baseline case, uniform velocity at the inlet of the pipe was given, while for pulsating flow cases, the following equation for imposing pulsation.

A very fine grid (10^{-5}) is employed near the wall to capture viscous and heat transfer effects correctly on the uniform velocity was employed as follows to obtain input pulsating velocity 14:

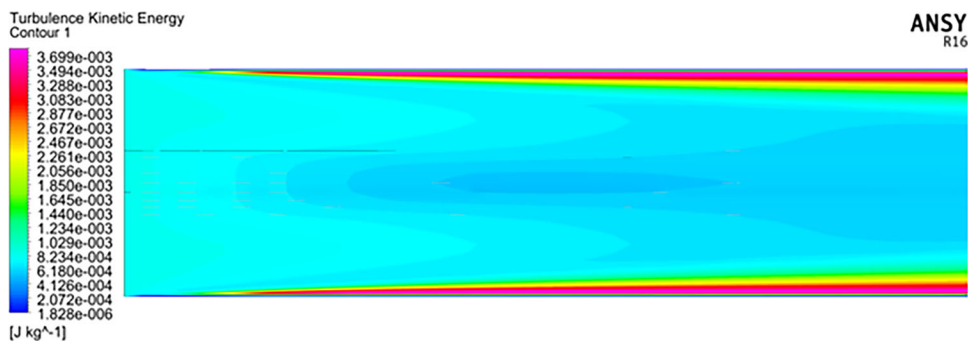
$$V = U_0[1 + A \sin(2\pi ft)] \quad (14)$$

where, U_0 is the non-pulsating velocity; A is the amplitude of pulsating flow; f is the frequency of pulsating flow and t represents time. Water is considered as the flowing fluid with Prandtl number, $Pr = 6.22$, dynamic viscosity of water, $\mu = 0.001 \text{ Pa} \cdot \text{s}$, specific heat capacity, $C_p = 3.732 \text{ kJ/kg} \cdot \text{K}$ and thermal conductivity, $K = 0.6 \text{ W/m} \cdot \text{k}$. Various sinusoidal pulsating velocity inputs with varied A s and f s are investigated. Figure 4 shows the velocity imposed at the inlet of the pipe with the different pulsation amplitude, A and $f = 0.3$. All the simulations are performed using ANSYS Fluent. Very high quality grids are generated with special care to grid metrics for the simulation. The orthogonality is close to 1 for the grid adopted for all the simulation. Due care is taken to resolve the boundary layer effects, by keeping near wall grid spacing of the order of 10^{-5} . Constant heat flux, Q is applied on the pipe wall during the simulations, while pressure-outlet condition is applied at the exit of the pipe.

3.4 Turbulent kinetic energy (TKE) analysis

One important factor affecting the improvement of heat transfer in pulsating flow is turbulent kinetic energy (TKE). Increased turbulence levels in pulsating flow regimes are caused by variations in pressure and velocity, which improve mixing and convective heat transfer. Elevated TKE concentrations enhance turbulent mixing, which facilitates heat transmission from the fluid to the adjacent surfaces. Compared to stable flow conditions, the periodic fluctuations in flow velocity lead to increased turbulence and higher heat

Fig. 5 TKE distribution near the inlet of the pipe for $Re = 12,000$, uniform velocity at inlet



transfer rates. Bergman et al. [12, 13], Tanda [74], Lind [48], Jin et al. [45]. TKE is an important parameter in fluid flow problems, which are turbulence dominated and involve heat transfer, which measures turbulence intensity and provides insight on the momentum, heat, and moisture transport through the boundary layer. Hence, it is very relevant to understand and thoroughly investigate the effects with respect to TKE analysis, as it has been well established that the turbulence aids heat transfer enhancement. By incorporating TKE analysis into investigations of pulsating heat transfer, researchers can gain a deeper understanding of the underlying fluid dynamics and heat transfer mechanisms, leading to the development of more efficient and reliable thermal management systems. Because of the inherent randomness of the typical chaotic system in the distribution of the number of vaporized cores, the speed of air plug rupture, the number of collisions of fluid microclusters, and the boiling time of fluid columns when the pipe is in its operating state, traditional analytical methods are unable to fully reveal the operating characteristics of the pulsating heat pipe Fan et al. [24].

Subtracting the equation for the mean (or base) flow from the equation for the instantaneous motion yields the equation for the fluctuation. Therefore, 15 depicts varying velocity.

$$\rho \left[\frac{\partial u_i}{\partial t} + U_{ij} \frac{\partial u_i}{\partial x_j} \right] = - \frac{\partial p}{\partial x_i} + \frac{\partial \tau_{ij}^v}{\partial x_j} - \rho \left[u_j \frac{\partial U_i}{\partial x_j} \right] - \left\{ u_j \frac{\partial u_i}{\partial x_j} - \rho \left\langle u_j \frac{\partial u_i}{\partial x_j} \right\rangle \right\} \quad (15)$$

where, τ_{ij} represents the stress tensor and the terms in $\langle \rangle$ bracket indicates time averaged convective term. When we look at the kind and nature of the components in this equation, we can see that the derivative of the fluctuating velocity, which represents the mean motion, is on the left-hand side. The variable pressure gradient and the fluctuating viscous stresses are represented by the first two terms on the RHS. The third item on the right-hand side is the source term, or so-called production term, which draws energy from the mean flow. The final term has a quadratic relationship to the

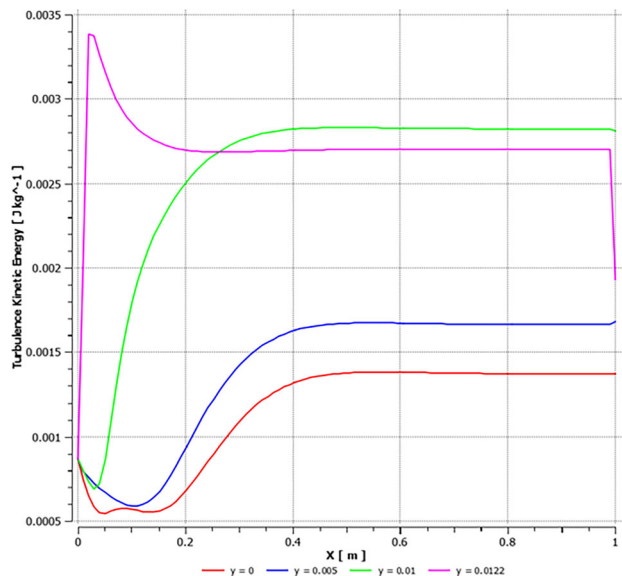


Fig. 6 TKE distribution at different radii of the pipe for $Re = 12,000$, uniform velocity at inlet

varying velocity. The bracketed term in the equation for the fluctuation vanishes if the disturbance is tiny or infinitesimal, leaving the equation to be linear in the disturbance. After taking scalar product of Eq. 16 with the fluctuating velocity itself and average, we get

$$\left[\frac{\partial}{\partial t} + U_j \frac{\partial}{\partial x_j} \right] k = \frac{\partial}{\partial x_j} \left\{ - \frac{1}{\rho} \langle p u_i \rangle \delta_{ij} - \frac{1}{2} \langle q^2 u_j \rangle + v \frac{\partial}{\partial x_j} k \right\} - \langle u_i u_j \rangle \frac{\partial U_i}{\partial x_j} - v \left\langle \frac{\partial u_i}{\partial x_j} \frac{\partial u_i}{\partial x_j} \right\rangle \quad (16)$$

These equations are crucial to the study of turbulence. The majority of second-order closure attempts at turbulence modeling are based on Eq. 15, while 16 offers the framework for understanding the dynamics of turbulent motion.

The contours of TKE for $Re = 12,000$, $Q = 15000W/m^2$ are as shown in Fig. 5. The variation of the TKE at different

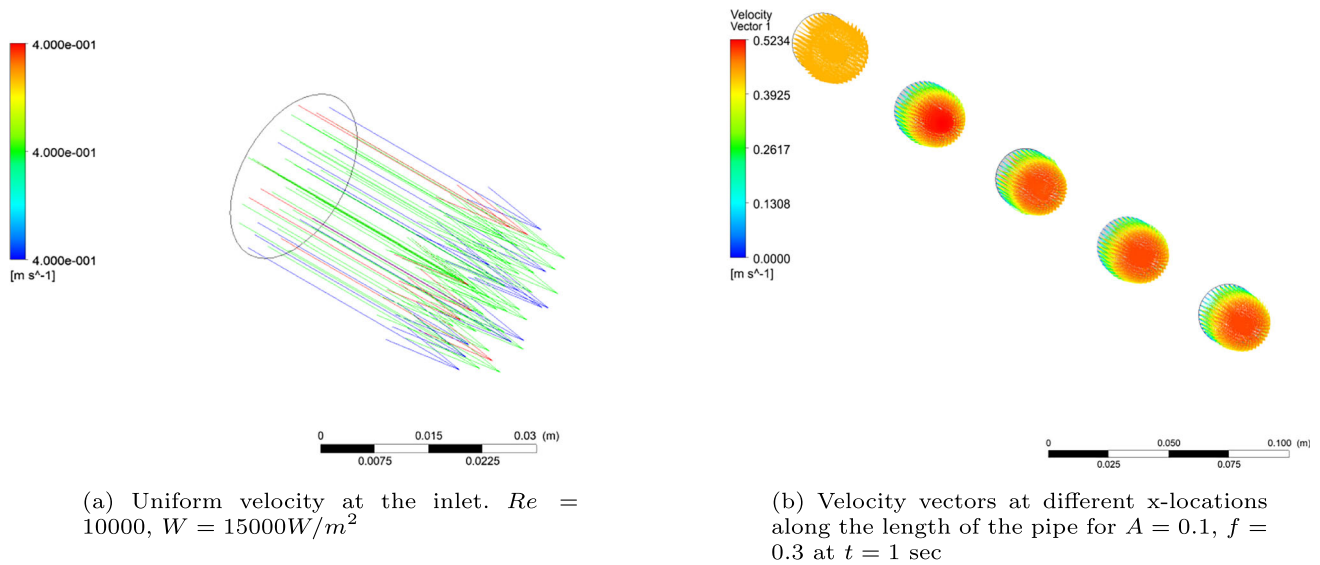


Fig. 7 Velocity vectors for two different sets of inlet velocity conditions. **a** Uniform velocity at the inlet. $Re = 10,000$, $W = 15000W/m^2$. **b** Pulsating velocity at inlet

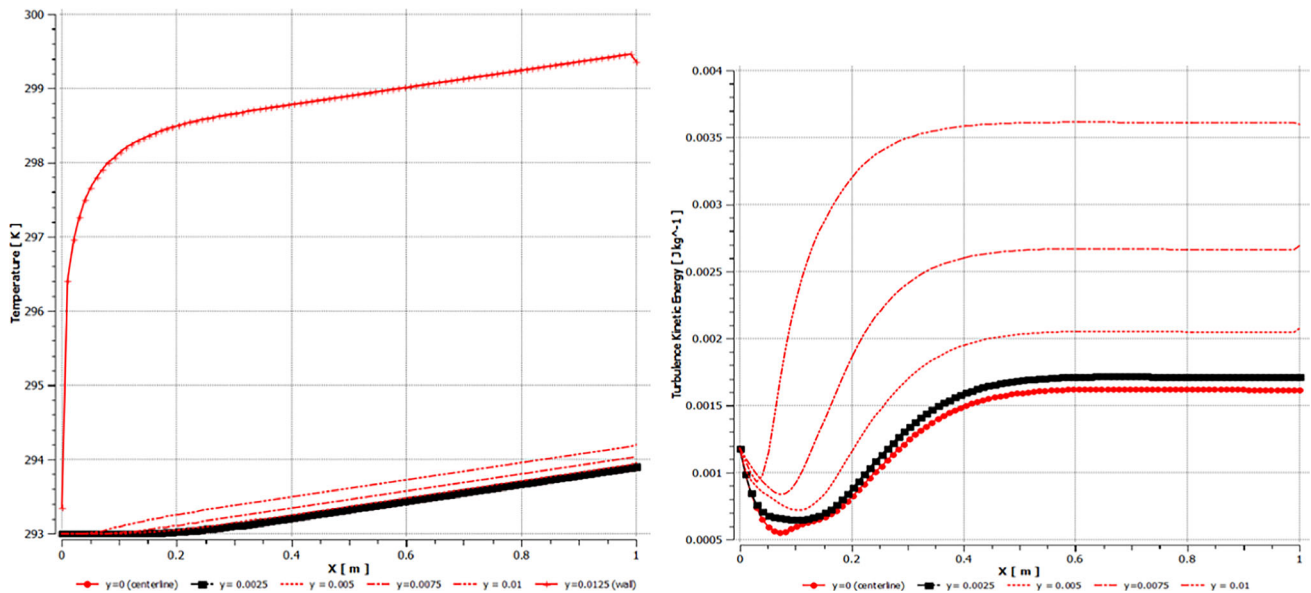


Fig. 8 Temperature and TKE distribution along the length of the pipe at different radii for $Re = 14,000$, uniform velocity at inlet case at $t = 6$ s

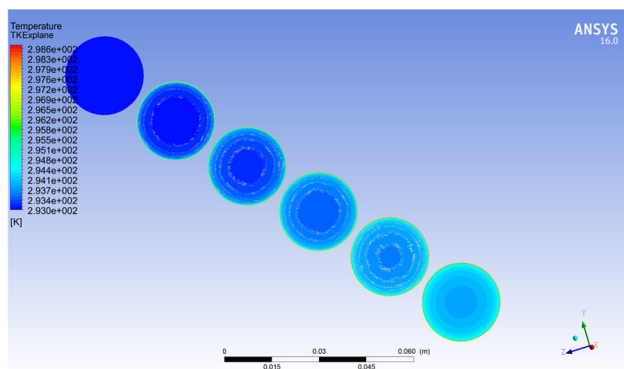
radii is as shown in Fig. 6 for this case. It is to be noted that the term indicates the rate of production of turbulence kinetic energy from the mean flow.

4 Results

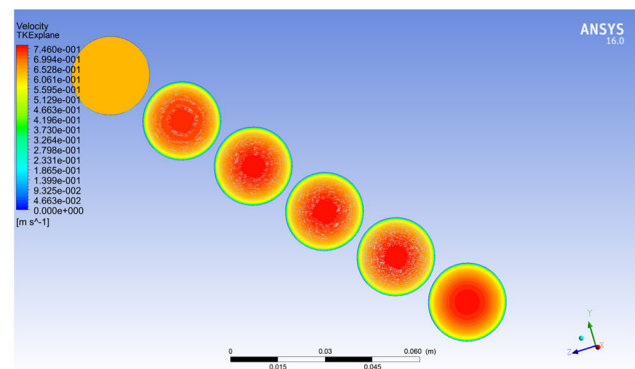
As reported by many researchers that heat transfer increases with increased Re , f and A Ye et al. [84] (and references therein), we have considered several parameters during the present investigation. In this section, comparative analysis is provided with respect to inflow condition, Re , L , D etc.

The initial analysis has been done for a baseline case with $Re = 10,000$, $D = 0.025$ m, $L = 1$ m without any pulsation. The computational results are compared with the theoretical solution. For this case, $Nu_{theoretical} = 75$ and $Nu_{comp} = 76$ have been obtained. Upon validation locations along the length of stigated by altering the values.

Figure 7a shows velocity vectors at the inlet of the pipe indicating uniform velocity at the inlet for the present case. All the velocity vectors are of equal length indicating uniform flow with constant magnitude at the inlet of the pipe, as it was imposed in the boundary condition. Figure 7b shows velocity vectors at different x-locations along the length of the pipe



(a) Temperature distribution at various sections along the length of the pipe.



(b) Spatial distribution of velocity at various sections along the length of the pipe.

Fig. 9 Spatial distribution of temperature and velocity for $Re = 16,000$, uniform velocity, $Q = 15000 \text{ W/m}^2$

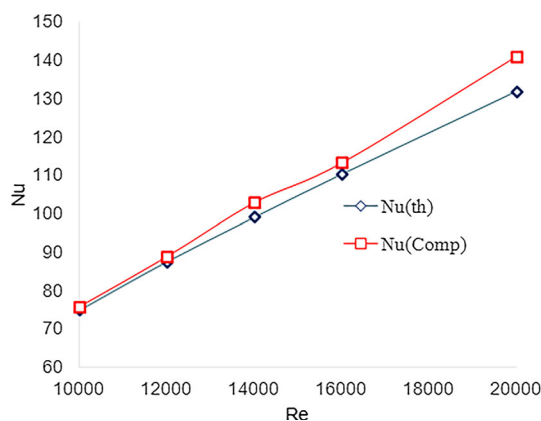


Fig. 10 Comparison of computed and theoretical Nu for different Re with uniform velocity at the inlet

for $A = 0.1$, $f = 0.3$. We note a paraboloid spread of velocity vectors at different x -locations along the length of the pipe (Fig. 7b).

Figure 6 shows turbulent kinetic energy distribution near the inlet of the pipe for $Re = 12,000$, uniform velocity at inlet. Wall is the main source for creating turbulence and hence the maximum TKE is noted close to the wall as shown in figure for $y = 0.0122 \text{ m}$. It is very important to note that for the radii in the vicinity of centreline the TKE follow a similar pattern, while for near wall we note a spike in the near entry region at $x = 0.05$. Effects of presence of the wall are predominant here. With length of the pipe the TKE is diffused in the flow domain and after $x = 0.4 \text{ m}$ TKE remains constant till the exit of the flow. This is due to the fact that the disturbances in the flow, which were created near the entrance of the pipe attenuate.

Figure 8 shows the Temperature and TKE distribution along the length of the pipe at different radii for $Re = 14,000$, uniform velocity at inlet case. It is noted that the TKE for all the radii initially surges from the inlet for some distance along

the length and then the magnitude increased till $x = 0.4 \text{ m}$. After $x = 0.4 \text{ m}$, the magnitude remains constant till the exit of the flow domain. This is different behaviour as compared to $Re = 12,000$ case, where TKE at different radius displayed different patterns. Observations on the effects of change in Re on heat transfer are noted as follows. Nusselt number is calculated based on the diameter of the pipe. $D = 0.025 \text{ m}$ at the turbulent length of the pipe at the exit of the flow domain. A comparison of theoretical and computed results is as shown in Fig. 10. The results obtained are in very good agreement with the theoretical results within a deviation of 6.9%. It is noted that as the Re increases, Nu also increases. The reason being higher Re flow possess higher kinetic energy, thereby creating higher turbulence, which aids in better heat transfer from the wall surface. However, it is to be noted that in the cases for $Re = 10,000$ – $20,000$, we have noted a velocity profile developing in the nearby region of the inlet. For all the cases investigated in this section, a uniform velocity was considered at the inlet of the pipe. The Re range considered is a completely turbulent regime.

Figure 9a shows temperature distribution at various sections along the length of the pipe (spatial variation) at $t = 6 \text{ s}$. It is noted that, as one goes from inlet to outlet the temperature in the core of the flow domain gradually increases till the outlet of the pipe. Similar observations were made for earlier cases also, the difference being the magnitude. Here, in this case the temperature increases to $T = 296 \text{ }^\circ\text{C}$, as compared to $T = 307 \text{ }^\circ\text{C}$ in $Re = 10,000$ case (figure now shown). Figure 9b shows spatial distribution of velocity at various sections along the length of the pipe. $Re = 16,000$, uniform velocity, $Q = 15000 \text{ W/m}^2$. A central core with higher velocity magnitude is found from $x = 0.2 \text{ m}$ till the exit of the flow domain. The velocity fluctuations are not observed to significant during this region (Fig. 10).

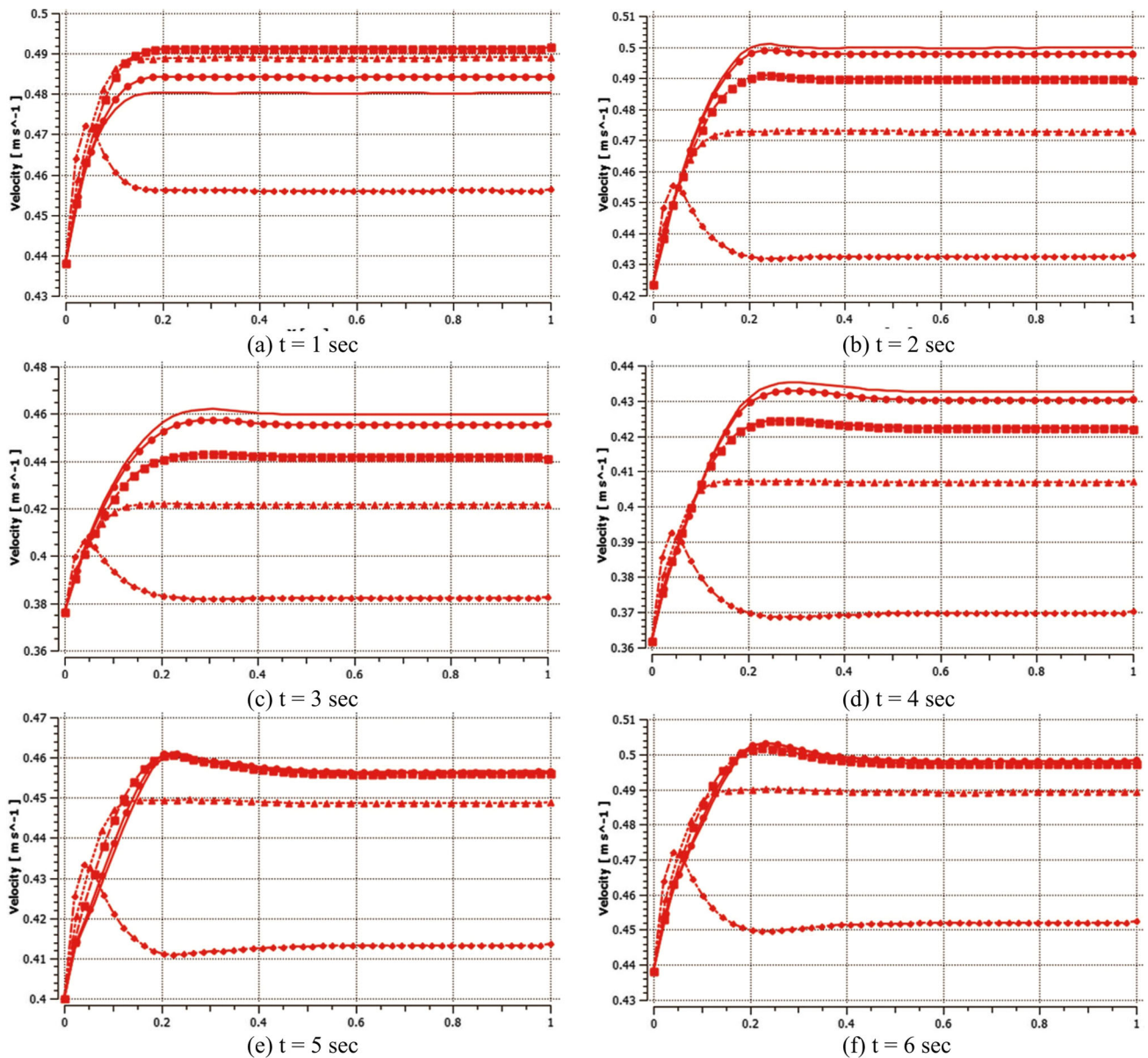


Fig. 11 Variation in velocity at different radii for $Re = 10,000$, $A = 0.1$, $f = 0.2$ at indicated times the flow domain $0.6 < x < 1.0$

Figures 11 and 12 show velocity variation at different times and TKE variation at different radii at $t = 6$ s respectively. The effect of pulsating velocity is quite evident from Fig. 11. A pulse is generated at every radius, effect of which is though observed till $x = 0.4$ m. The velocity pulses created at different radii at the same time creates a wave front, which encourages turbulence in the flow field. For the low amplitude $A = 0.1$ and frequency, $f = 0.2$, the pulse is seen to create a disturbance till half of the domain. It is to be noted that for every time instance, the velocity magnitude changes drastically at a given radius. This change in the velocity magnitude creates a puff-like structure which penetrates in the flow domain with higher kinetic energy.

Figure 13 shows TKE contours at different x – locations along the length of the pipe for $A = 0.1$, $f = 0.3$ in the whole domain. It is noted that the source for the TKE generation is wall, which incepts turbulence from the inlet of the pipe. In the inlet region TKE in the flow domain has less intensity and has the maximum intensity in the later part of the domain (about $0.6 < x < 0.8$ m) and gradually decreased till the exit of the domain. Figure 14 shows variation in velocity at various radii at different times for $Re = 10,000$, $L = 1$ m, $A = 0.1$, $f = 0.3$. With increases in frequency from $f = 0.2$ to 0.3 , the velocity profile drastically changes and the velocity wave front become strong with varied maxima. At different locations and different times, the velocity magnitude change

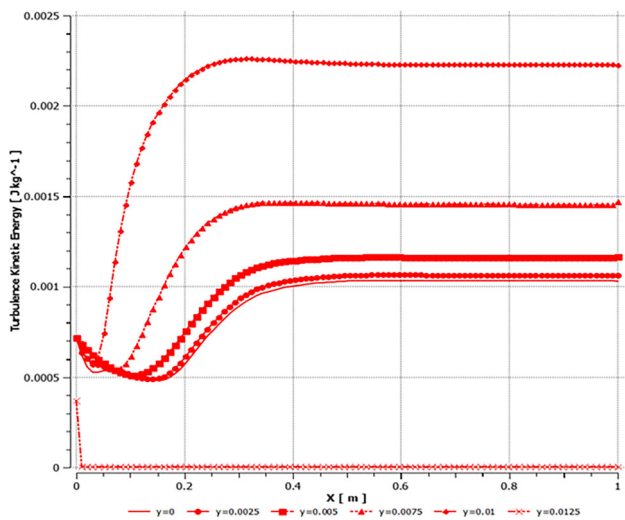


Fig. 12 TKE variation at different radii at $t = 6$ s

is significant, effects of which are also noted in TKE contours. Similarly velocity centreline velocity profiles for this case at different times are shown in Fig. 15. One can note the velocity pulse and wave front created in the flow domain with time. This pulse encouraged turbulence in the flow field. However, it to be noted that the effect is not significant in later part of.

In this later half of the length of the pipe the velocity at different radii almost remains constant. Figure 16 shows variation in velocity at various radii at different times for $Re = 10,000, L = 1$ m, $A = 0.1, f = 0.4$. Very interesting observations are made in this case. With increases in frequency from $f = 0.3$ to 0.4 , the velocity profile drastically changes and the velocity wave front become strong with varied maxima. At different locations and different times, the velocity magnitude change is significant. The velocity profiles at various radii and time instances indicates that several wave fronts are created in the domain and the turbulence is augmented with a combination of such impulses. Figure 17 shows velocity distribution near inlet of the pipe for $Re = 10,000, A = 0.2, f = 0.4$. It is quite evident from the figure that at this combination of A and f , the flow near the inlet is significantly affected. Different contours indicated that the pulsation has penetrated inside the domain quite well. The maximum velocity noted for this case at $t = 6$ s is 0.5188 m/s.

Fig. 13 TKE contours at different x – locations along the length of the pipe for $A = 0.1, f = 0.3$

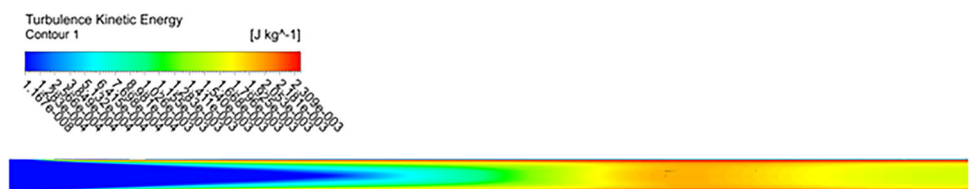


Figure 18 shows the summary of effect of change in length on Nu . For all the three cases of different lengths, time instantaneous Nu undulates, depending upon the f and A of the pulsation. The corresponding dotted lines shows the linear fit of the individual curve. It is noted that after 2 s, the time instantaneous Nu for $L = 1$ is bit higher than other two lengths, $L = 1.5$ and 2 m. For the longest pipe, the time instantaneous Nu is the lowest. However, it is to be noted that change in time- averaged Nu for these three case is not significant. It can be concluded that the length of the pipe does not make any significant effect on heat transfer characteristics. Figure 19 shows effect of change in diameter on Nu . It is clearly seen from the variation of the Nu that for the smallest diameter $D = 0.02$ m, time instantaneous Nu is the least, while for the largest diameter, $D = 0.03$ m, corresponding magnitudes are the maximum. Dotted lines indicate the linear fit for each curve. It is observed that during initial transits, the Nu is on higher side, however with lapse of time ($t = 3$ s), the Nu oscillates about a mean value. The corresponding Nu for these cases are shown in Fig. 20. The results obtained are in very good agreement with the theoretical results. As seen this figure, from graph we can see that according to change in amplitude there is slight difference of as amplitude changes, at some point that is at 2 s we can see that it is overlapping; it is due to effect of pulsation. But we can observe that if we take average of all, with respect to time at each amplitude, is approximately same after comparing for all amplitude means it is increasing in very minor range with respect to amplitude.

Figure 21 shows the comparison of theoretical and computed Nu for $Re = 10,000, f = 0.3$ Hz and $A = 0.2$. Initially there is difference of 12% between theoretical value and numerical computed value but as we compute for longer time then the matches to the theoretical value as we can see at $t = 3$ s. Is much closer that is 2%. Initially there is difference, however for later times it matches to theoretical value with minor difference.

4.1 Effects of change in Reynolds number

The results are obtained for $Re = 10,000, 12,000, 14,000, 16,000$ and $20,000$ (see Fig. 10). With increase in Re , heat transfer is enhanced, due to high kinetic energy of the fluid at high Re . It is noted that despite of pulsating velocity input,

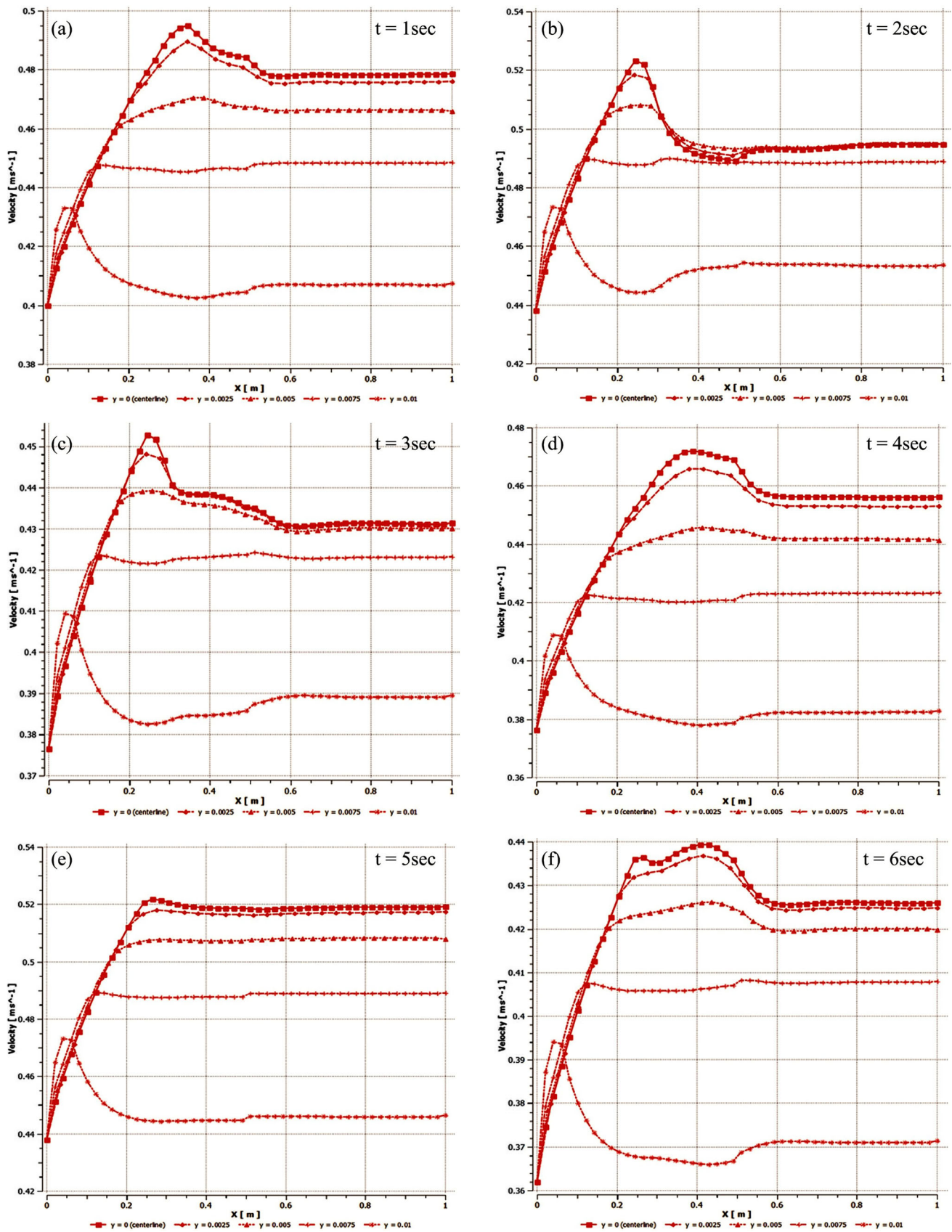


Fig. 14 Variation in velocity at various radii at different times for $Re = 10,000, L = 1 \text{ m}, A = 0.1, f = 0.3$

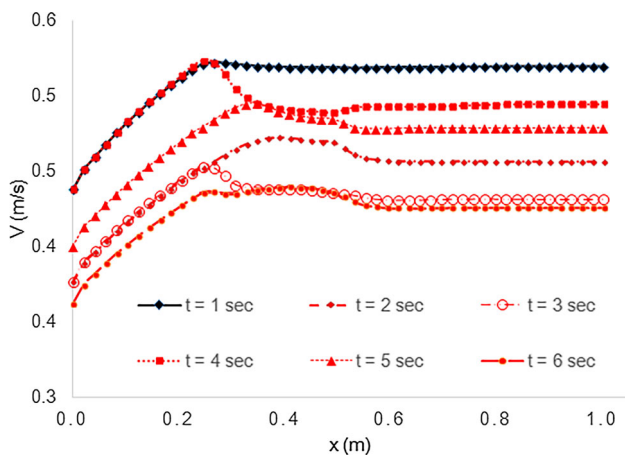


Fig. 15 Centreline velocity at different times for $Re = 10,000$, pulsating velocity, $A = 0.1$, $f = 0.3$

there is no significant heat transfer enhancement for the considered range of As and fs . This fact has also been reported by several other researchers. Hence, it is imperative to understand the mechanism through which this objective can be achieved. Through this study, we have made this attempt by analysing the turbulent kinetic energy, which is a good measure of diffusion of the energy transport in the flow domain. It is noted that the effect of the pulsation sustains in a part of the flow domain, and a major part near the outlet does not get affected by this pulsation adequately. Other cases investigated for understanding the effects of change in Re are reported in Table 1.

4.2 Effects of change in amplitude and frequency of pulsation

It is noted that higher frequency pulsating velocity inputs penetrate into the domain at a farther distance, thereby providing enhancement in local Nu as compared to low frequencies. However, one needs to investigate a large range of such frequency inputs to find out an optimum combination with amplitude.

Though the time instantaneous Nu shows the nature similar to input velocity pulse, when we perform time-averaging, the time-averaged Nu is found to be close to the case without any pulsating velocity input.

Table 2 shows consolidated results of other cases investigated for studying the effects of change in A and f . It is to be noted that the Nu_{Th} values are obtained using Eq. (13), which does not take into account A and f .

4.3 Effect of change in length of the pipe

For the three cases of different lengths, time instantaneous Nu is found to be undulating about a mean value, depending

upon the f and A of the pulsation. For the longest pipe, the time instantaneous Nu is the lowest. However, it is to be noted that change in time-averaged Nu for these three cases is not significant.

It is noted that higher frequency pulsating velocity inputs penetrate into the domain at a farther distance, thereby providing enhancement in local Nu_{local} , as compared to low frequencies. However, one needs to investigate a large range of such frequency inputs to find out an optimum combination with amplitude. Though the time instantaneous Nu shows the nature similar to input velocity pulse, when we perform time-averaging, the time-averaged Nu is found to be close to the case without any pulsating velocity input. It can be concluded that the length of the pipe does not make any significant effect on heat transfer characteristics.

Table 3 shows the effect of L for $Re = 10,000$, $V = 0.4$ m/s, $A = 0.2$, $f = 0.3$.

4.4 Effect of change in diameter of the pipe

The smallest diameter $D = 0.02$ m, time instantaneous Nu is the least, while for the largest diameter, $D = 0.03$ m, corresponding magnitudes are found to be maximum. It is observed that during initial transits, the Nu is on the higher side, however with lapse of time ($t = 3$ s), the Nu oscillates about a mean value.

Table 4 shows the effect of diameter of pipe for $L = 1$ m, $A = 0.2$, $f = 0.3$.

5 Conclusions

In the present research, we have thoroughly investigated the mechanism of heat transfer for turbulent flows. It has been a well-accepted fact that turbulence aids the heat transfer process. Many researchers have attempted to enhance it by providing pulsating velocity input at the inlet of the flow domain. We have investigated the mechanism for a circular pipe with varying various parameters. Various cases have been investigated with the aim to investigate the effects of different parameters like Re , amplitude (A) and frequency of pulsating inlet velocity (f), length of pipe (L), diameter of pipe, (D) for a given constant heat flux, (Q) on the pipe wall. In the present research work, we have limited the Re range from 10,000 to 20,000 and fs and As considered were also of low magnitude. The present research on the increase of heat transfer via pulsating flow in a straight circular pipe has provided insightful information about the intricate interactions between several elements. This study clarifies the effects of variables such as pulsation amplitude, frequency, diameter, pipe length, and Re on heat transfer characteristics, with a particular emphasis on TKE, by methodically investigating these aspects. The

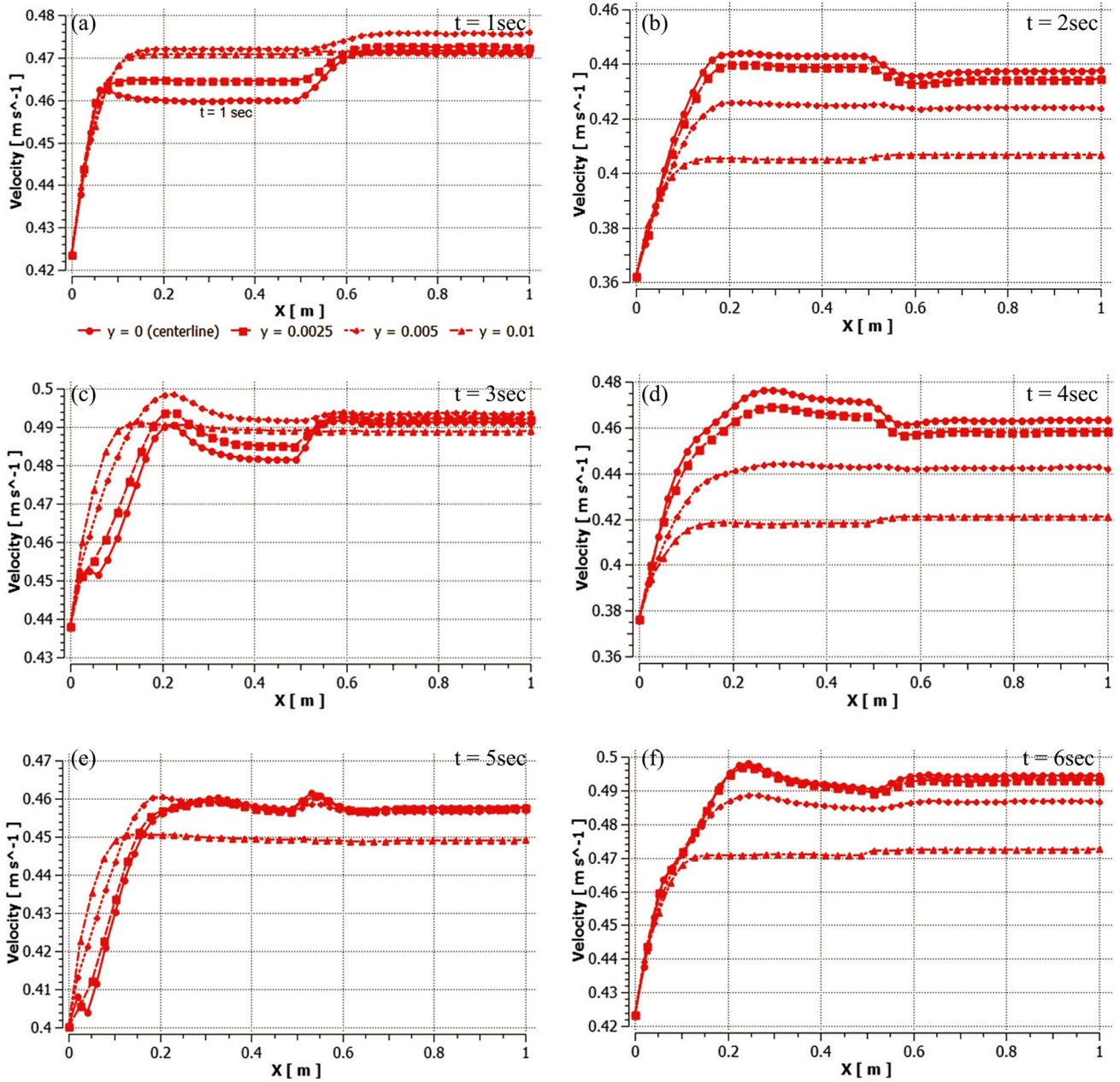
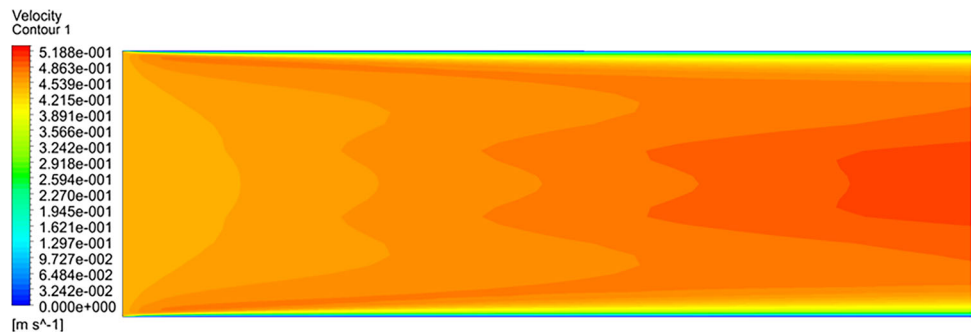


Fig. 16 Variation in velocity at various radii at different times for $Re = 10,000, L = 1 \text{ m}, A = 0.1, f = 0.4$

Fig. 17 Velocity distribution near inlet of the pipe for $Re = 10,000, A = 0.2, f = 0.4$ at $t = 6 \text{ s}$



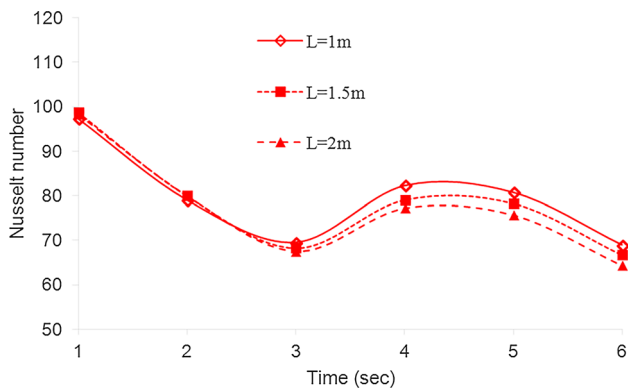


Fig. 18 Effect of change in length on Nusselt number, Nu

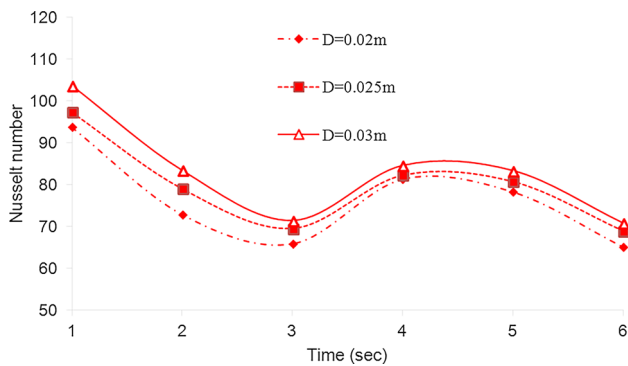


Fig. 19 Effect of change in diameter of the pipe on Nusselt number, Nu

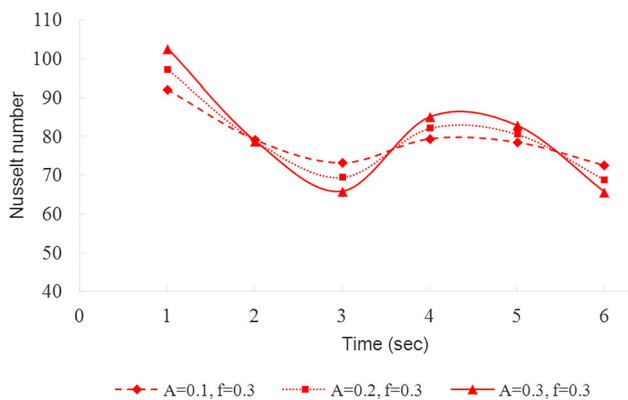


Fig. 20 Computed Nusselt number (Nu) for various amplitudes and $f = 0.3$ Hz

TKE analysis is reported which provides insight into flow development and its effects on the heat transfer enhancement.

It has been noted that, owing to larger kinetic energy with a higher Re , heat transfer is improved as Re increases. However, throughout the examined range of A 's and f 's, no discernible improvement of heat transfer was seen, even in the presence of pulsating velocity inputs. Higher frequency pulsations travel farther within the domain and produce higher local Nusselt numbers than lower frequencies. The

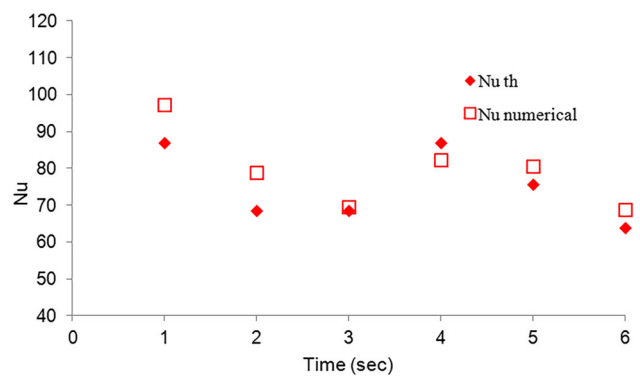


Fig. 21 Comparison of theoretical and numerical Nu for $Re = 10,000$, $A = 0.2$ and $f = 0.3$ Hz

Table 1 Effect of Re without pulsating velocity ($D = 0.025$ m, $L = 1$ m)

S.N	Re	Vel (m/s)	NuTh	NuComp
1	10,000	0.4	75	76
2	12,000	0.4808	87.61	89
3	14,000	0.561	99.12	103
4	16,000	0.64115	110.29	113.3
5	20,000	0.8	131.84	141

time-averaged Nusselt number, on the other hand, stayed quite near to the scenario without pulsating velocity input, indicating that more research across a wider frequency range is required to identify the best pairings with amplitude. Similar experimental analysis was also carried out by Alimohammadi et al. [5] As for the effects of pipe diameter and length, our research shows that although these variables affect time instantaneous Nusselt numbers, they have no discernible effect on timeaveraged values. This shows that, within the confines of our study, the pipe's length and diameter do not significantly change the properties of heat transfer. Future studies will examine a broader range of Re , f and A , while taking into account the overall wave's steepness and size in forced convective heat transfer mechanisms subjected to pulsing flow circumstances.

In convective heat transfer, higher frequency pulsing velocity inputs cause a rise in the local Nusselt number relative to low frequencies. This effect results from the complex interaction between the properties of the fluid flow and the mechanisms of thermal transport in the boundary layer near the solid surface. The fluid undergoes quick oscillations in flow velocity at higher frequencies of pulsing velocity inputs, which causes dynamic changes in the boundary layer structure Bauer et al. [11], Schlichting [66]. Increased turbulence and improved mixing inside the boundary layer caused by the intensified fluid motion close to the solid surface improve convective heat transfer efficiency by improving

Table 2 Effect of pulsation amplitude and frequency ($Re = 10,000$, $D = 0.025$ m, $L = 1$ m)

S.N	f	A	NuTh	NuComp
1	0.2	0.1	75	77.258
2	0.3	0.1	75	76.6098
3	0.4	0.1	75	79.4538
4	0.2	0.2	75	76.8705
5	0.3	0.2	75	76.08754
6	0.4	0.2	75	77.5647
7	0.2	0.3	75	77.0474
8	0.3	0.3	75	75.6778
9	0.4	0.3	75	77.78678

Table 3 Effect of Length of pipe ($Re = 10,000$, $V = 0.4$ m/s, $A = 0.2$, $f = 0.3$)

S.N	Length (m)	NuTh	NuComp
1	1.0	75	76.00978
2	1.5	75	74.41372
3	2.0	75	72.87584

Table 4 Effect of diameter of pipe for $L = 1$ m, $A = 0.2$, $f = 0.3$

S.N	Re	Vel. m/s	Dia. (m)	NuTh	NuComp
1	7985.6	0.4	0.02	63	61.5831
2	10,000	0.4	0.025	75	76.08918
3	10,000	0.333	0.03	75	79.42482
4	10,000	0.5	0.02	75	73.49768

fluid–solid interaction and raising heat transfer rates. Many spatial and temporal scales are displayed by the developing flow Sengupta [68]. Smaller temporal and spatial fluid motion scales brought about by higher frequency pulsations cause the boundary layer's turbulent structures to form at a finer scale. Heat transport is aided by the higher dissipation rates of these smaller-scale turbulent eddies. More of a fluid–solid surface interaction is produced by the boundary layer's dynamic reaction to high-frequency velocity pulsations. The fluid entrainment from the outer flow areas into the boundary layer is facilitated by this improved contact.

6 Future scope

It has been noted that creating turbulence in the flow field helps in heat transfer enhancement. This has been investigated both experimentally and numerically by several

researchers. Both small scale and large scale perturbations are responsible for such phenomenon. Lighthill [47] investigated such small amplitude effects on the boundary layer. He expressed the oncoming flow in the exponential form. Such investigation at a varied range of Re can be conducted with reference to heat transfer enhancement studies. Also studies on effect of by-pass transition Sengupta [67] on heat transfer enhancement can be undertaken. Investigation on heat transfer enhancement with different forms of inserts, vortex generators and effect of secondary flow is part of our future work. Kholi et al. [42] reported pulsating heat transfer applications in various thermal domains and developed semi-empirical correlations for pulsating heat transfer using ANN models for prediction. Also, the present investigation can be further extended for turbomachinery applications and developing interactive design models for nano-fluids employed in pulsating heat transfer. During the present investigation, the focus has been made on the effects of various parameters on the heat transfer enhancement. The present study utilized velocity, temperature distribution and TKE analysis for reporting the effects. However, the present study is limited to a lower range of Re $7000 < Re < 20,000$ and the limited range of lower values of frequencies and amplitudes of pulsation. A rigorous investigation on the effects of such parameters with an increased range of Re , A and f is suggested to probe into the details of the physics. Despite of the fact that some efforts have been made in this regard, there is a need for a thorough investigation. This can be taken up as future study to find the trend and limitations of such pulsating flow behaviour.

References

1. Akdag, U., Ozdemir, M.: Heat transfer in an oscillating vertical annular liquid column open to atmosphere. *Heat Mass Transfer* **42**, 617–624 (2006). <https://doi.org/10.1007/s00231-005-0035-0>
2. Akdag, U., Ozdemir, M.: Heat removal from oscillating flow in a vertical annular channel. *Heat Mass Transfer* **44**, 393–400 (2008). <https://doi.org/10.1007/s00231-007-0248-5>
3. Akdag, U., Oztug, A.F.: Experimental investigation of heat transfer in oscillating annular flow. *Int. J. Heat Mass Transf.* **52**(11), 2667–2672 (2009). <https://doi.org/10.1016/j.ijheatmasstransfer.2009.01.006>
4. Alami, A.H., Ramadan, M., Tawalbeh, M., Haridy, S., Al Abdulla, S., Aljaghoub, H., Ayoub, M., Alashkar, A., Abdelkareem, M.A., Olabi, A.G.: A critical insight on nanofluids for heat transfer enhancement. *Sci. Rep. Nat. Portfolio* **13**, 15303 (2023). <https://doi.org/10.1038/s41598-023-42489-0>
5. Alimohammadi, S., Kumavat, P.S., O'Shaughnessy, S.M.: An experimental-numerical study of heat transfer enhancement in a minichannel using asymmetric pulsating flows. *IEEE Trans. Compon., Packag. Manuf. Technol.* **13**(8), 3299085 (2023). <https://doi.org/10.1109/TCPMT.2023>
6. Aljibory, M.W., Alais, S.M., Rashid, F.L.: An Experimental and Numerical Investigation of Heat Transfer Enhancement Using Annular Ribs in a Tube. In: *IOP Conf. Series: Materials Science*

- and Engineering, vol. 433, p. 012057. (2018). <https://doi.org/10.1088/1757-899X/433/1/012057>.
7. Ashwin, V.M., Saurabh, K., Sriramkrishnan, M., Bagade, P.M., Parvathi, M.K., Sengupta, T.K.: KdV equation and computations of solitons: nonlinear error dynamics. *J. Sci. Comput.* **62**(3), 693–717 (2015). <https://doi.org/10.1007/s10915-014-9875-4>
 8. Babu, E.R., Reddy, N.C., Babbar, A., Chandrashekar, A., Kumar, R., Bains, P.S., Alsubih, M., et al.: Characteristics of pulsating heat pipe with variation of tube diameter, filling ratio, and SiO₂ nanoparticles: biomedical and engineering implications. *Case Stud. Therm. Eng.* **55**, 104065 (2024). <https://www.sciencedirect.com/science/article/pii/S2214157X24000960>
 9. Bagade, P.M., Bhumkar, Y.G., Sengupta, T.K.: An improved orthogonal grid generation method for solving flows past highly cambered aerofoils with and without roughness elements. *Comput. Fluids* **103**, 275–289 (2014). <https://doi.org/10.1016/j.compfluid.2014.07.031>
 10. Balje, O.E.: A study on reynolds number effects in turbomachines. *J. Eng. Power* (1964). <https://doi.org/10.1115/1.3677584>
 11. Bauer, W.-D., Wenisch, J., Heywood, J.B.: Averaged and time-resolved heat transfer of steady and pulsating entry flow in intake manifold of a spark-ignition engine. *Int. J. Heat Fluid Flow* **19**(1), 1–9 (1998)
 12. Bergman, T.L., Incropera, F.P., Lavine, A.S., Dewitt, D.P.: *Fundamentals of Heat and Mass Transfer*, VII John Wiley and Son, Hoboken (2011). ISBN: 13 978-0470-50197-9: 401
 13. Bergman, T.L., Lavine, A.S., Incropera, F.P., DeWitt, D.P.: *Introduction to heat transfer*. John Wiley & Sons, Hoboken (2011)
 14. Chattopadhyay, H., Durst, F., Ray, S.: Analysis of heat transfer in simultaneously developing pulsating laminar flow in a pipe with constant wall temperature. *Int. Commun. Heat Mass Transfer* **33**, 475–481 (2006). <https://doi.org/10.1016/j.icheatmasstransfer.2005.12.008>
 15. Chen, C., Gao, P., Tan, S., Yu, Z.: Boiling heat transfer characteristics of pulsating flow in rectangular channel under rolling motion. *Exp. Therm Fluid Sci.* **70**, 246–254 (2016). <https://www.sciencedirect.com/science/article/pii/S0894177715002502>
 16. Chen, Z., Utaka, Y., Tasaki, Y.: Measurement and numerical simulation on the heat transfer characteristics of reciprocating flow in microchannels for the application in magnetic refrigeration. *Appl. Therm. Eng.* **65**(1), 150–157 (2014)
 17. Constantinou, H., Lani, S., Rouaze, G., Thome, J.R.: High Performance Pulsating Heat Pipe for Electronics Cooling. In: 2022 21st IEEE Intersociety Conference on Thermal and Thermomechanical Phenomena in Electronic Systems (iTherm), pp 1–9 (2022)
 18. Cumpsty, N.A., Greitzer, E.M.: A simple model for compressor stall cell propagation. *J. Eng. Power* **104**(1), 170–176 (1982). <https://doi.org/10.1115/1.3227246>
 19. Daba, R., Xu, S., Wang, W., Huang, Y., Luo, X., Fang, K.: Effect of flow pulsation on heat transfer performance of biomimetic bark microchannel heat sink. *Case Stud. Therm. Eng.* **56**, 104255 (2024)
 20. Dittus, F.W., Boelter, L.M.K.: Heat transfer in automobile radiators of the tubular type. *Int. Commun. Heat Mass Transfer* **12**(1), 3–22 (1985). [https://doi.org/10.1016/0735-1933\(85\)90003-X](https://doi.org/10.1016/0735-1933(85)90003-X)
 21. Elshafei, E.A., Mohamed, M.S., Mansour, H., Sakr, M.: Numerical Study of Heat Transfer in Pulsating Turbulent Air Flow. In: 2007 International Conference on Thermal Issues in Emerging Technologies: Theory and Application, pp. 63–70. <https://doi.org/10.1109/THETA.2007.363411>(2007)
 22. Elshafei, E.A.M., Safwat Mohamed, M., Mansour, H., Sakr, M.: Experimental study of heat transfer in pulsating turbulent flow in a pipe. *Int. J. Heat Fluid Flow* **29**(4), 1029–1038 (2008). <https://doi.org/10.1016/j.ijheatfluidflow.2008.03.018>
 23. Esfe, H., Mohammad, M.B., Torabi, A., Valadkhani, M.: A critical review on pulsating flow in conventional fluids and nanofluids: thermo-hydraulic characteristics. *Int. Commun. Heat Mass Transfer* **120**, 104859 (2021). <https://doi.org/10.1016/j.icheatmasstransfer.2020.104859>
 24. Fan, Y., Wang, Z., Guo, J., Ma, D., Yang, W.: Capture of kinetic behavior of ethanol-based copper oxides in pulsating heat pipe. *Int. J. Heat Mass Transfer* **225**, 125392 (2024). <https://www.sciencedirect.com/science/article/pii/S0017931024002230>
 25. Gbadebo, S.A., Said, S.A.M., Habib, M.A.: Average Nusselt number correlation in the thermal entrance region of steady and pulsating turbulent pipe flows. *Heat Mass Transf.* **35**, 377–381 (1999). <https://doi.org/10.1007/s002310050339>
 26. Gerrard, J.H.: An experimental investigation of pulsating turbulent water flow in a tube. *J. Fluid Mech.* **46**(1), 43–64 (1971). <https://doi.org/10.1017/S0022112071000399>
 27. Ghafarian, M., Mohebbi-Kalhari, D., Sadegi, J.: Analysis of heat transfer in oscillating flow through a channel filled with metal foam using computational fluid dynamics. *Int. J. Therm. Sci.* **66**, 42–50 (2013). <https://doi.org/10.1016/j.ijthermalsci.2012.11.008>
 28. Gül, H.: Experimental investigation of heat transfer in oscillating circular pipes: high frequencies and amplitudes. *Sci. Res. Essays* **8**(13), 524–531 (2013). <https://doi.org/10.5897/SRE12.721>
 29. Guo, Z., Sung, H.J.: Analysis of the Nusselt number in pulsating pipe flow. *Int. J. Heat Mass Transfer* **40**(10), 2486–2489 (1997). [https://doi.org/10.1016/S0017-9310\(96\)00317-1](https://doi.org/10.1016/S0017-9310(96)00317-1)
 30. Han, J.-C., Chen, H.-C.: Turbine blade internal cooling passages with rib turbulators. *J. Propul. Power* **22**(2), 226–248 (2006). <https://doi.org/10.2514/1.12793>
 31. Han, J.-C., Wright, L.: *Analytical Heat Transfer*, II CRC Press, Boca Raton (2022). <https://doi.org/10.1201/9781003164487>
 32. Havemann, H.A., Narayan Rao, N.N.: Heat transfer in pulsating flow. *Nature* **174**, 41 (1954). <https://doi.org/10.1038/174041a0>
 33. He, S., Jackson, J.D.: An experimental study of pulsating turbulent flow in a pipe. *Eur. J. Mech. B. Fluids* **28**(2), 309–320 (2009). <https://doi.org/10.1016/j.euromechflu.2008.05.004>
 34. Hemida, H.N., Sabry, M.N., Abdel-Rahim, A., Mansour, H.: Theoretical analysis of heat transfer in laminar pulsating flow. *Int. J. Heat Mass Transf.* **45**(8), 1767–1780 (2002). [https://doi.org/10.1016/S0017-9310\(01\)00274-5](https://doi.org/10.1016/S0017-9310(01)00274-5)
 35. Hengeveld, D., Mathison, M., Braun, J., Groll, E., Williams, A.: Review of modern spacecraft thermal control technologies. *HVACR Res.* **16**, 189–220 (2010)
 36. Hosseinalipour, S.M., Shahbazian, H., Sunden, B.: Coriolis and buoyancy effects on heat transfer in viewpoint of field synergy principle and secondary flow intensity for maximization of internal cooling. *Heat Mass Transfer* **57**, 1467–1483 (2021). <https://doi.org/10.1007/s00231-020-02949-z>
 37. Hota, S.K., Lee, K.-L., Leitherer, B., Elias, G., Hoeschele, G., Rökkam, S.: Pulsating heat pipe and embedded heat pipe heat spreaders for modular electronics cooling. *Case Stud. Therm. Eng.* **49**, 103256 (2023). <https://www.sciencedirect.com/science/article/pii/S2214157X23005622>
 38. Jun, Z., Danling, Z., Ping, W., Hong, G.: An experimental study of heat transfer enhancement with a pulsating flow. *Heat Transfer—Asian Res.* **33**(5), 279–286 (2004). <https://doi.org/10.1002/htj.20020>
 39. Kern, D.Q.: *Process Heat Transfer*, p. 43. McGraw Hill International Book Company, New York (1983)
 40. Khandekar, S., Charoensawan, P., Groll, M., Terdtoon, P.: Closed loop pulsating heat pipes - Part B: visualization and semi-empirical modeling. *Appl. Therm. Eng.* **23**, 2021–2033 (2003)
 41. Kharvani, H.R., Zohir, A.E., Doshmanziari, F.I., Jalali-Vahid, D.: An experimental investigation of heat transfer in a spiral-coil tube with pulsating turbulent water flow. *Heat Mass Transfer* **52**, 1779–1789 (2016). <https://doi.org/10.1007/s00231-015-1697-x>
 42. Kholi, F.K., Park, S., Yang, J.S., Ha, M.Y., Min, J.K.: A detailed review of pulsating heat pipe correlations and recent advances using

- artificial neural network for improved performance prediction. *Int. J. Heat Mass Transfer* **207**, 124010 (2023). <https://www.sciencedirect.com/science/article/pii/S0017931023001631>
43. Khosravi-Bizhaem, H., Ravan, A.Z., Abbassi, A.: Heat transfer enhancement and pressure drop by pulsating flow through helically coiled tube: an experimental study. *Appl. Therm. Eng.* **160**, 114012 (2019). <https://doi.org/10.1016/j.applthermaleng.2019.114012>
 44. Kikuchi, Y., Suzuki, H., Kitagawa, M., Ikeya, K.I.: Effects of pulsating strouhal number on heat transfer around a heated cylinder in pulsating cross-flow. *JSME Int. J. Ser. B* **43**(2), 250–257 (2000). <https://doi.org/10.1299/jsmeb.43.250>
 45. Lee, J., Sung, H.J., Jung, S.Y., Zaki, T.A.: Effect of wall heating on turbulent boundary layers with temperature-dependent viscosity. *J. Fluid Mech.* **726**, 196–225 (2013). <https://doi.org/10.1017/jfm.2013.211>. <https://koasas.kaist.ac.kr/bitstream/10203/174103/1/000319736300009.pdf>
 46. Leong, K.C., Jin, L.W.: Characteristics of oscillating flow through a channel filled with open-cell metal foam. *Int. J. Heat Fluid Flow* **27**(1), 144–153 (2006). <https://doi.org/10.1016/j.ijheatfluidflow.2005.05.004>
 47. Lighthill, M.J.: On sound generated aerodynamically. I. general theory. *Proc. Roy. Soc. Lond. Ser. A, Math. Phys. Sci.* **211**(1107), 564–587 (1952). Accessed 26 Mar 2024. <http://www.jstor.org/stable/98943>.
 48. Lind, E.K.: Analysis of turbulence models in a cross flow pin fin microheat exchanger. PhD diss., Monterey, Calif. Naval Postgraduate School (2002)
 49. Lohrasbi, S., Hammer, R., Essl, W., Reiss, G., Defregger, S., Sanz, W.: A comprehensive review on the core thermal management improvement concepts in power electronics. *IEEE Access* **8**, 166880–166906 (2020)
 50. Mackley, M.R., Tweddle, G.M., Wyatt, I.D.: Experimental heat transfer measurements for pulsatile flow in baffled tubes. *Chem. Eng. Sci.* **45**(5), 1237–1242 (1990). [https://doi.org/10.1016/0009-2509\(90\)87116-A](https://doi.org/10.1016/0009-2509(90)87116-A)
 51. Magerramova, L., Vasilyev, B., Kinzburskiy, V.: Novel Designs of Turbine Blades for Additive Manufacturing. *Turbo Expo: Power for Land, Sea, and Air 5C: Heat Transfer*, pp. 2021–2033 (2016). <https://doi.org/10.1115/GT2016-56084>
 52. McAdams, W.H.: *Heat Transmission*, 3rd edn. McGraw-Hill, New York (1954)
 53. Metwally, M.: Review of Compressible Pulsating Flow Effects on System Performance. In: 13th International Conference on Aerospace Sciences and Aviation Technology, ASAT- 13 (2009). <https://doi.org/10.21608/asat.2009.23729>.
 54. Miao, J.J., Wang, R.H., Jian, T.W., Hsu, Y.T.: An investigation into inflection-point instability in the entrance region of a pulsating pipe flow. *Proc. R Soc. A* (2016). <https://doi.org/10.1098/rspa.2016.0590>
 55. Mladin, E.-C., Zumbrennen, D.A.: Alterations to coherent flow structures and heat transfer due to pulsations in an impinging air-jet. *Int. J. Therm. Sci.* **39**(2), 236–248 (2000). [https://doi.org/10.1016/S1290-0729\(00\)00242-8](https://doi.org/10.1016/S1290-0729(00)00242-8)
 56. Moschandreou, T., Zamir, M.: Heat transfer in a tube with pulsating flow and constant heat flux. *Int. J. Heat Mass Transf.* **40**(10), 2461–2466 (1997). [https://doi.org/10.1016/S0017-9310\(96\)00266-9](https://doi.org/10.1016/S0017-9310(96)00266-9)
 57. Mu, H., Shi, W.: Review of operation performance and application status of pulsating heat pipe. *Sustainability* **16**(7), 2722 (2024). <https://www.mdpi.com/2071-1050/16/7/2722>
 58. Nabavi, M.: Steady and unsteady flow analysis in microdiffusers and micropumps: a critical review. *Microfluid. Nanofluid.* **7**, 599–619 (2009). <https://doi.org/10.1007/s10404-009-0474-x>
 59. Nabavi, M.: Invited review article: unsteady and pulsating pressure and temperature: a review of experimental techniques. *Rev. Sci. Instrum.* **81**(3), 031101 (2010). <https://doi.org/10.1063/1.3327886>
 60. Nishandar, S.V., Pawar, P.B., Dabhole, A.S., Patil, P.B., Kulkarni, P.D.: Experimental investigation of heat transfer characteristics of pulsating flow in a pipe. *Int. J. Theor. Appl. Res. Mech. Eng. (IJTARME)* (2018). <https://doi.org/10.2991/978-94-6463-136-427>
 61. Nobrega, G., Cardoso, B., Souza, R., Pereira, J., Pontes, P., Catarino, S.O., Pinho, D., Lima, R., Moita, A.: A review of novel heat transfer materials and fluids for aerospace applications. *Aerospace* **11**(4), 275 (2024). <https://www.mdpi.com/2226-4310/11/4/275>
 62. Persoons, T., Saenen, T., Donose, R., Baelmans, M.: Heat transfer enhancement due to pulsating flow in a microchannel heat sink. In: 2009 15th International Workshop on Thermal Investigations of ICs and Systems, pp. 163–167. (2009). <https://api.semanticscholar.org/CorpusID:11440811>.
 63. Plotnikov, L.V.: Unsteady gas dynamics and local heat transfer of pulsating flows in profiled channels mainly to the intake system of a reciprocating engine. *Int. J. Heat Mass Transfer* **195**, 123144 (2022). <https://www.sciencedirect.com/science/article/pii/S00179310220006159>
 64. Ryley, J.R., McGilvray, M., Gillespie, D.: Local Heat transfer coefficient measurements on an engine representative internal cooling passage. *AIAA* (2019). <https://doi.org/10.2514/1.T5206>
 65. Saha, A.D., Mahmood, F.T., Smriti, R.B., Sumon, H., Hasan, M.N.: CFD analysis of heat transfer enhancement by wall mounted flexible flow modulators in a channel with pulsatile flow. *Heliyon* **9**, e16741 (2023). <https://doi.org/10.1016/j.heliyon.2023.e16741>
 66. Schlichting, H.: *Turbulence and heat stratification*. Technical Report (1950)
 67. Sengupta, T.K.: *Instabilities of Flows and Transition to Turbulence*. CRC Press, Boca Raton (2012). ISBN: 3: 978-1-4398-7945-0
 68. Sengupta, T.K.: *Instabilities of Flows and Transition to Turbulence*. Taylor & Francis, Francis (2012)
 69. Sheriff, H.S., Zumbrennen, D.A.: Effect of flow pulsations on the cooling effectiveness of an impinging jet. *J. Heat Transfer* **116**(4), 886–895 (1994). <https://doi.org/10.1115/1.2911463>
 70. Shu, M., Qing, D., Wang, H.: Study on heat transfer performance of pulsating flow in convergent-divergent tube. *IOP Conf. Ser.: Earth Environ. Sci.* **153**, 032023 (2018). <https://doi.org/10.1088/1755-1315/153/3/032023>
 71. Sierra-Vargas, G., Garzon-Alvarado, D., Duque-Daza, C.: The effects of mainstream reynolds number and blowing ratio on film cooling of gas turbine vanes. *Fluids* **8**, 263 (2023). <https://doi.org/10.3390/fluids8100263>
 72. Singh, S.K., Mali, H.S., Suryawanshi, S., Singh, S.: Pulsed flow microchannel heat sink: simulation and experimental validation. *J. Micromanufacturing* **5**(1), 29–35 (2022). <https://doi.org/10.1177/25165984211058625>
 73. Sobhnamayan, F., Sarhaddi, F., Behzadmehr, A.: Analytical solution of pulsating flow and forced convection heat transfer in a pipe filled with porous medium. *J. Comput. Appl. Mech.* **52**(4), 570–587 (2021). <https://doi.org/10.22059/jcamech.2021.327163.638>
 74. Tanda, G.: Effect of rib spacing on heat transfer and friction in a rectangular channel with 45 angled rib turbulators on one/two walls. *Int. J. Heat Mass Transf.* **54**(5–6), 1081–1090 (2011)
 75. Targui, N., Kahalerras, H.: Analysis of a double pipe heat exchanger performance by use of porous baffles and pulsating flow. *Energy Convers. Manage.* **76**, 43–54 (2013). <https://doi.org/10.1016/j.enconman.2013.07.022>
 76. Tesa, V., Trávníček, Z.: Pulsating and synthetic impinging jets. *J. Visualization* **8**, 201–208 (2005). <https://doi.org/10.1007/BF03181497>
 77. Wagshul, M.E., Eide, P.K., et al.: The pulsating brain: a review of experimental and clinical studies of intracranial pulsatility. *Fluids and Barriers of the CNS* **8**(1), 5 (2011). <https://doi.org/10.1186/2045-8118-8-5>

78. Wang, X., Zhang, N.: Numerical analysis of heat transfer in pulsating turbulent flow in a pipe. *Int. J. Heat Mass Transf.* **48**(19), 3957–3970 (2005). <https://doi.org/10.1016/j.ijheatmasstransfer.2005.04.011>
79. Wilcox, D.C., et al.: *Turbulence modeling for CFD*, vol. 2. DCW industries, La Canada (1998)
80. Winterton, R.H.S.: Technical notes: where did the Dittus and Boelter equation come from. (1998) <https://api.semanticscholar.org/CorpusID:91685561>
81. Wu, L., Chen, J., Wang, S.: Experimental study on thermal performance of a pulsating heat pipe using R1233zd(E) as working fluid. *Int. Commun. Heat Mass Transfer* **135**, 106152 (2022). <https://www.sciencedirect.com/science/article/pii/S0735193322002743>
82. Wu, H.-W., Lay, R.F., Lau, C.T., Wu, W.-J.: Turbulent flow field and heat transfer in a heated circular channel under a reciprocating motion. *Heat Mass Transfer* **40**(10), 769–778 (2004). <https://doi.org/10.1007/s00231-003-0464-6>
83. Xiao, G., Chen, C., Shi, B., Cen, K., Ni, M.: Experimental study on heat transfer of oscillating flow of a tubular Stirling engine heater. *Int. J. Heat Mass Transf.* **71**, 1–7 (2014). <https://doi.org/10.1016/j.ijheatmasstransfer.2013.12.010>
84. Ye, Q., Zhang, Y., Wei, J.: A comprehensive review of pulsating flow on heat transfer enhancement. *Appl. Therm. Eng.* **196**, 117275 (2021). <https://doi.org/10.1016/j.applthermaleng.2021.117275>
85. Yu, J.-C., Li, Z.-X., Zhao, T.S.: An analytical study of pulsating laminar heat convection in a circular tube with constant heat flux. *Int. J. Heat Mass Transf.* **47**(24), 5297–5301 (2004). <https://doi.org/10.1016/j.ijheatmasstransfer.2004.06.029>
86. Yuan, Bo., Zhang, Y., Liu, L., Wei, J., Yang, Y.: Experimental research on heat transfer enhancement and associated bubble characteristics under high-frequency reciprocating flow. *Int. J. Heat Mass Transf.* **146**, 118825 (2020). <https://doi.org/10.1016/j.ijheatmasstransfer.2019.118825>
87. Zhao, T., Cheng, P.: A numerical solution of laminar forced convection in a heated pipe subjected to a reciprocating flow. *Int. J. Heat Mass Transf.* **38**(16), 3011–3022 (1995). [https://doi.org/10.1016/0017-9310\(95\)00017-4](https://doi.org/10.1016/0017-9310(95)00017-4)
88. Zohir, A.E., Habib, M.A., Attya, A.M., Eid, A.I.: An experimental investigation of heat transfer to pulsating pipe air flow with different amplitudes. *Heat Mass Transfer* **42**(7), 625–635 (2006). <https://doi.org/10.1007/s00231-005-0036-z>

Publisher's Note Springer Nature remains neutral with regard to jurisdictional claims in published maps and institutional affiliations.

Springer Nature or its licensor (e.g. a society or other partner) holds exclusive rights to this article under a publishing agreement with the author(s) or other rightsholder(s); author self-archiving of the accepted manuscript version of this article is solely governed by the terms of such publishing agreement and applicable law.